Inversion of Large-scale ZTEM Data

Elliot Holtham
UBC-Geophysical Inversion Facility
Dept. of Ocean and Earth Sciences
University of British Columbia
6449 Stores Rd
Vancouver, BC V6T 1Z4, Canada
eholtham@eos.ubc.ca

Douglas W. Oldenburg
UBC-Geophysical Inversion Facility
Dept. of Ocean and Earth Sciences
University of British Columbia
6449 Stores Rd
Vancouver, BC V6T 1Z4, Canada
doug@eos.ubc.ca

SUMMARY

As the number of near surface deposits decreases, it becomes increasingly important to develop geophysical techniques to image at depth. Because of the penetration advantage of plane wave natural sources, these techniques are ideal to answer questions about the deep subsurface to the earth. A ZTEM survey is an airborne electromagnetic survey which records the vertical magnetic field that result from natural sources. The data are transfer functions that relate the local vertical field to orthogonal horizontal fields measured at a reference station on the ground. While the airborne nature of the survey means that large survey areas can be surveyed quickly and economically, the high number of cells required to discretize the entire survey area at reasonable resolution can make the computational costs of inverting the entire data set all at once prohibitively expensive. Here we present a workflow methodology that can be used to invert large natural source surveys by decomposing the large inverse problem into smaller more manageable problems before combining the tiles into a final inversion result. We use the procedure to invert synthetic ZTEM data for the Noranda mining camp as well as a field data example. Both of these data sets were far too large to solve on a single grid even with multiple processors at our disposal.

Key words: inversion, electromagnetics, airborne EM

INTRODUCTION

Since most shallow and outcropping deposits have already been discovered, many of the earth's remaining natural resources are buried deep in the subsurface and they are difficult to find. In order to satisfy the strong global resource demand, techniques to explore for these big targets at depth must be developed. Electromagnetic methods can be used to map electrical conductivity which can then be linked to geologic features of interest. When exploring for large, deeply buried targets, natural source electromagnetic methods can be advantageous over controlled source methods because of the deeper penetration of plane wave sources.

The traditional natural source method, the magnetotelluric (MT) method, has been effectively applied to both mining and hydrocarbon exploration. A practical limitation of the MT technique is that surveys are costly and time consuming because many expensive stations must be installed to measure the needed electromagnetic field components on the earth's surface. It would be preferable to collect MT data in an aircraft but this goal has not yet been achieved because of the difficulty in measuring the electric fields. In an effort to continue to use the penetration advantage of natural sources, it has long been recognized that tipper data, the ratio of the local vertical magnetic field to the horizontal magnetic field, provide information about 3D electrical conductivity structure. It was this understanding that prompted the development of AFMAG (Audio Frequency Magnetics) (Ward, 1959). However, because the direction and strength of the inducing field varies with time, AFMAG results were not always repeatable. Limitations of the AFMAG technique were outlined in (Ward et al., 1966).

Many of the AFMAG problems can be removed by using improved signal processing and instrumentation. This has resulted in the Z-Axis Tipper Electromagnetic Technique (ZTEM) (Lo and Zang, 2008). In ZTEM, the vertical component of the magnetic field is recorded above the entire survey area, while the horizontal fields are recorded at a ground-based reference station. MT processing techniques yield frequency domain transfer functions typically between 30-720 Hz that relate the vertical fields over the survey area to the horizontal fields at the reference station. Since new instrumentation exists to measure the vertical magnetic fields by helicopter, data over large survey areas can quickly be collected. The result is a cost effective procedure for collecting natural source EM data that provide information about the 3D conductivity structure of the earth.

On the district and regional scale, particularly when the subsurface geology is hidden under cover, high quality airborne data sets are excellent exploration tools. For example large ZTEM surveys, in excess of 5000 line-km of data, have been collected. However, in order to justify spending significant money on collecting such data, interpretation methods must be capable of inverting the data in a reasonable amount of time. This requires that inversions are fairly fast, especially for field data where multiple inversions are often performed using different parameters. Unfortunately, for surveys that cover large areas and where even moderate resolution is desired, the discrete 3D Maxwell systems for solving the EM problem quickly become very large. Although computer technology continues to improve, clock speed and instruction level parallelism has started to flatten since 2003 (Shalf, 2007). This means that the majority of future improvements in the size of inverse problem that can be tackled must come from improved methodologies and increased parallelism.

One viable method to solve large inverse problems is to reduce the modelling domain by using footprint methods, where computations are simplified by only considering model cells that influence the data above some threshold criterion. These methods have been used to invert large airborne controlled source electromagnetic data sets (Cox et al., 2010) and MT data sets (Gribenko et al., 2010). Another solution is to use domain decomposition methods (DDM) and split the computational domain into smaller manageable subproblems which can then be solved quickly in parallel. In this paper we present a highly parallel and effective workflow procedure to invert large natural source surveys.

ZTEM DATA

ZTEM data are transfer functions that relate the vertical magnetic fields computed above the earth to the horizontal magnetic field at some fixed reference station. This relation is given by

$$H_z(r) = T_{zx}(r, r_0)H_x(r_0) + T_{zy}(r, r_0)H_y(r_0) \quad (1)$$

where r is the location for the vertical field, r_0 is the location of the ground based reference station and are the vertical field transfer functions. Solving for the transfer functions requires that the vertical fields are known for two independent polarizations.

INVERSION METHODOLOGY

Our MT inversion algorithm is that of (Farquharson et al., 2002), and our ZTEM inversion algorithm is that of (Holtham and Oldenburg 2008) and (Holtham and Oldenburg, 2010). We wish to solve the inverse problem by minimizing the objective function

$$\min \phi = \left\| \mathbf{W}_d (F(\mathbf{m}) - \mathbf{d}) \right\| + \beta \phi_m , \quad (2)$$

where $\mathbf{W}_d$ is a diagonal measurement weighting matrix, $\square_m$ is the model objective function, F is the forward modelling operator which acts on the model **m**, and **d** is the data vector. Although the goal is to solve this problem, it is difficult to tackle directly because of the size of the problem and the cost of evaluating F(**m**). While the full inverse problem may be too expensive to solve, coarsely discretized models can be solved quickly and efficiently.

We first start by decomposing the model domain, **m,** and the data set, **d**, into smaller subdomains,

$$\begin{aligned} \mathbf{m}_j &= P^m{}_j \mathbf{m}, j = 1,...J, \\ \mathbf{d}_j &= P^d{}_j \mathbf{d}, j = 1,...J, \end{aligned} \quad (3)$$

where $P^m{}_i$ and $P^d{}_i$ are projection operators which form the model and data subdomains respectively. Here $P^m{}_i$ is constructed such that the $\mathbf{m}_i$'s are overlapping. We would like to invert these subproblems separately and in parallel but there are interactions between subdomains that cannot be ignored. In order to mitigate this problem we determine the first order interactions between domains by performing a coarse inversion and then use the computed fields as source terms for the subdomain inversions. That is, first we obtain a coarse inversion result $\mathbf{m}_c$ by inverting the entire data set on the coarse mesh. The coarse model is then interpolated onto the J subdomains to create initial models. The electric fields obtained by forward modelling the coarse conductivity structure, are also interpolated onto the J domains. Although these new fields are only defined on individual subdomains, they still contain information about the full conductivity structure. These electric fields are used as the primary fields when carrying out an inversion on each subdomain. By using a primary-secondary field formulation and using primary fields computed from a global scale model, the correct large-scale physics of the problem is maintained.

Once all of the individual subdomain models, $\mathbf{m}_i$'s have been determined, an update to the full model **m** is given by merging each subdomain into a final full conductivity structure. To ensure that this new result is acceptable, the predicted data from this full fine scale model is computed. If the data misfit is acceptable, then a solution to the desired inverse problem has been obtained. If the data have not been sufficiently fit, then new fields generated by this new inversion result can be used as the primary fields for another iteration of subdomain inversions. This procedure can be repeated until the data has been sufficiently fit.

SYNTHETIC EXAMPLE

In this section a synthetic model is used to examine in detail a few elements of the general methodology described in the previous section. The synthetic model is from the Noranda District in Canada, home to 20 economic volcanogenic massive sulphide deposits (VMS), 19 orogenic Au deposits, and several intrusion-hosted Cu-Mo deposits (Gibson and Galley 2007). The original model provided courtesy of the Xstrata mining group contained 12.7 million cells covering an area of almost 20 x 20 km. The 38 geologic units in the model were converted into expected conductivities, before the entire 12.7 million cell model was forward modelled at 30, 45, 90, 180, 360 and 720Hz, and then corrupted with noise to form the observed synthetic data. A depth slice at -275m of the synthetic model can be seen in figure 3.

PRELIMNARY COARSE INVERSION

The first step in attempting to find an approximate solution to the full inverse problem is to perform a coarse inversion to determine the large scale conductivity structure that will be used to compute the primary fields and starting models for subsequent finer cell size inversions. The earth is discretized into relatively large cells such that the total number of cells in the mesh is small and the inverse problem can be solved quickly. In this example the coarse mesh contained 42 x 42, 500m cells in the x and y directions. It contained 73 cells in the z direction. Working initially on a coarse mesh, which for this synthetic example can be inverted in approximately 30 minutes, allows multiple inversions to be simultaneous run with different parameters and starting models. Because of the large cell dimensions, some geologic structures such as accurate body boundaries and fine scale features may not be recovered by the discretization. Therefore it is important not to overfit the data and risk adding discretization artifacts into the inversion result. This is particularly true for higher frequency data which will have smaller skin depths and contain more information about fine scale features. In fact, because the initial goal of the coarse scale inversion is to quickly determine the large scale conductivity features, some data, particularly the higher frequency data may be omitted to reduce the computational cost and prevent the large cell sizes of the coarse mesh from violating the shorter skin depths at the higher frequencies. In this example the 360 Hz and 720 Hz data were omitted for the coarse mesh inversion.

SETUP AND SUB-DOMAIN INVERSIONS

The coarse inversion result is used as an initial starting model and for computing the primary fields for subsequent finer discretized inversions. Once this is completed the subdomain meshes must be designed. When decomposing the computational domain and designing the subdomain meshes, the two critical elements pertain to handling the interactions between the domains and ensuring that there is continuity of conductivity structures across domain boundaries. Incorporating domain interactions is done by using primary fields in the tiled inversions which have been computed from full domain conductivity structures. Continuity of the conductivity structure across domain boundaries is accomplished by using both data and mesh overlap. Generally the meshes are chosen to overlap by slightly less than a skin depth at the lower frequencies. Here a tradeoff must be achieved between increased overlap and increased computational requirements. Another tradeoff that must be considered is the number of tiles used to decompose the domain. As the number of tiles increases, while the individual inversion time for each subproblem might decrease, the percentage of overlap cells versus total number of cells in each mesh increases and the decomposition may become less efficient. Here it is up to the user to choose a reasonable number of tiles such that each tile runs efficiently on their available computer hardware.

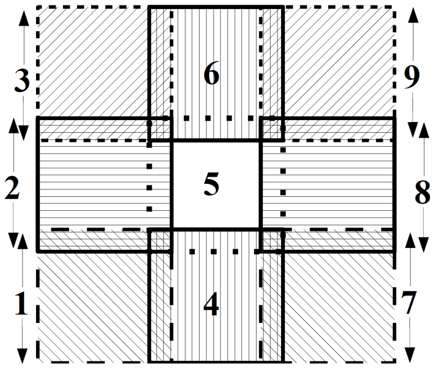

Figure 1 Mesh layouts for the example using nine overlapping domains. Each mesh contained approximately 1.4 million cells with 139 x 140 x 70 cells in the x,y and z directions. Each domain overlapped by 20, 50m cells in both the x and y directions.

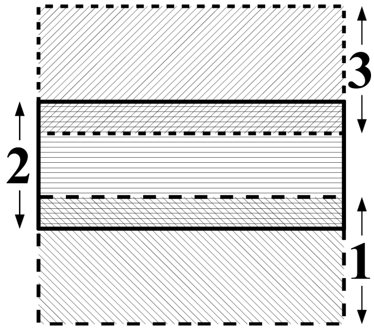

Figure 2 Mesh layouts for the example using three overlapping domains. Each subdomain mesh contained approximately 3.5 million cells with 353 x 140 x 70 cells in the x,y and z directions. Each domain overlapped by twenty 50m cells

For this synthetic example, two different sets of meshes, one with three tiles and the other with nine tiles are used to demonstrate the scalability and robustness of the methodology. Both the 3 and 9 tile examples contained the same sized cells (50 x 50 m cells in the x and y directions) in the core and overlapping regions. In the vertical direction the cells dimensions started at 25m, and then expanded with depth. Both sets of meshes used 20 overlapping cells on each mesh boundary. The mesh layouts and overlaps for the three and nine tile examples can be seen in figures 1 and 2.

Once the tiled models are inverted they are stitched together using a linear distance weighted averaging scheme across the overlapping regions. The final inversion models from the 3 and 9 tile examples in figures 4 and 5 recovers the large scale geological features very well. In addition several of the larger known deposits which were not evident from the in initial coarse inversion result are imaged. Here the inversion results of the 3 and 9 tile examples, run on dual Xeon X5660 processors, are very similar. This illustrates that the inversion results are not highly dependent on the choice of subdomain meshes. During the subdomain inversions the initial beta is chosen to be the final beta from the initial coarse inversion result and the same cooling scheme is used on the tiled inversions as in the initial coarse inversion.

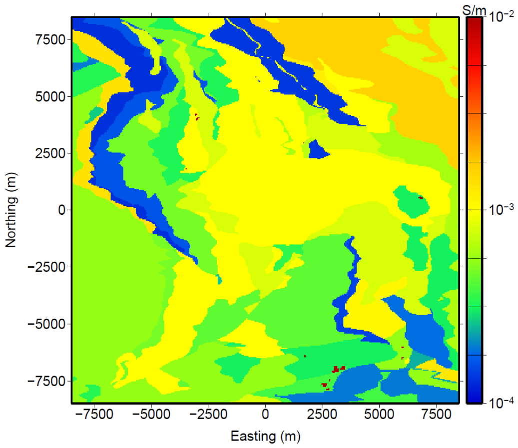

Figure 3 Depth slice at -275m of the true model. The topography for the synthetic model ranges from -25m to -250m. The conductivity of the ore was chosen to be 5 Ωm; however, the color scale on the model has been clipped at 100 Ωm to improve the visualization of the other geologic units.

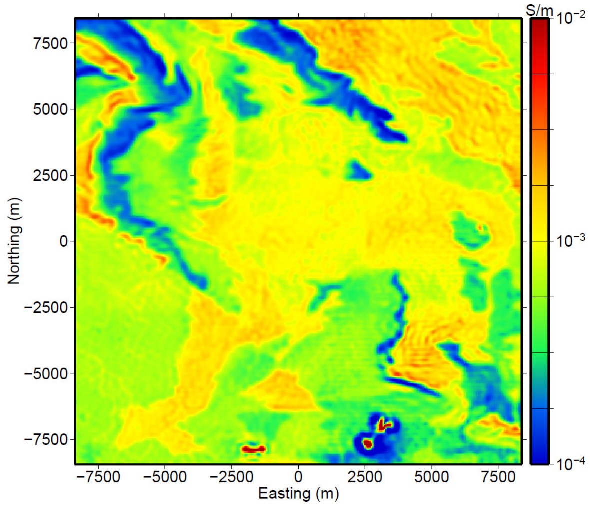

Figure 4 Depth slice at -275m of the inversion result after merging the three tiles together shown on the same color scale as the true model. The resolution in this model is greatly improved compared to the coarse result. Several of the larger known deposits have now been recovered; they were not visible from the initial coarse inversion.

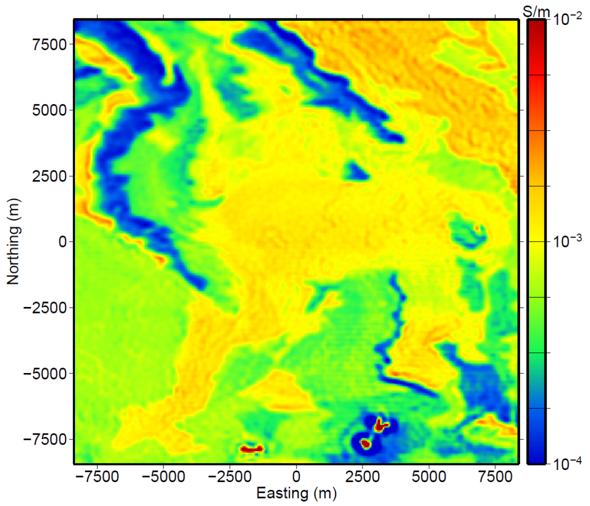

Figure 5 Depth slice at -275m of the inversion result after merging the 9 tiles together shown on the same color scale as the true model.

CONCLUSIONS

In this paper we show how large scale ZTEM survey data can be inverted by using a strategy involving coarse and fine meshes as well as a domain decomposition that splits the computational domain into smaller manageable subproblems which can be solved in parallel. We have presented a practical workflow procedure to carry this out. The methodology shows promising results on a synthetic example from the Noranda mining camp, and on a field data example that is currently being worked on.

ACKNOWLEDGEMENTS

The authors would like to thank the Mike Allard from Xstrata Zinc, Louis Martin from Xstrata Copper and Gervais Peron from Mira Geosciences, for providing the geologic shape model for the Noranda mining camp that has formed the basis of our synthetic example.

REFERENCES

Cox, L. H., G. A. W., and M. S. Zhdanov, 2010, 3d inversion of airborne electromagnetic data using a moving footprint: Exploration Geophysics, 41, 250–259.

Farquharson, C. G., D. W. Oldenburg, E. Haber, and R. Shekhtman, 2002, An algorithm for the three-dimensional inversion of magnetotelluric data: 72nd Annual International Meeting, SEG, Expanded Abstracts, 649–652.

Gibson, H., and A. Galley, 2007, Gibson, h., and galley, a.g, in Mineral Deposits of Canada: A Synthesis of Major Deposit-Types, District Metallogeny, the Evolution of Geological Provinces: Mineral Deposits Division, 5, 533–552.

Gribenko, A., A. G. M. C. M. Z., 2010, Efficient 3d inversion of mt data using integral equations method and the receiver footprint approach: application to the large-scale inversion of the earthscope mt data: Expanded Abstracts Denver.

Holtham, E., and D. Oldenburg, 2008, Three-dimensional forward modelling and inversion of z-tem data: SEG Extended Abstracts, Las Vegas.

———, 2010, Three-dimensional inversion of ztem data: Geophysical Journal International, 182, 168–182.

Lo, B., and M. Zang, 2008, Numerical modeling of z-tem (airborne afmag) responses to guide exploration strategies: SEG Technical Program Expanded Abstracts, 27, 1098–1102.

Shalf, J., 2007, The new landscape of parallel computer architecture: Journal of Physics: Conference Series, 78.

Ward, S. H., 1959, Afmag—airborne and ground: Geophysics, 24, 761–787.

Ward, S. H., J. O'Donnell, R. Rivera, G. H. Ware, and D. C. Fraser, 1966, Afmag - applications and limitations: Geophysics, 31, 576–605.